JOC*Article*

Liquid-Crystalline Bisadducts of [60]Fullerene

Stéphane Campidelli,[†] Ester Vázquez,[||] Dragana Milic,[†] Julie Lenoble,[§] Carmen Atienza Castellanos,[‡] Ginka Sarova,[‡] Dirk M. Guldi,*[,‡] Robert Deschenaux,*[,§] and Maurizio Prato*[,†]

Dipartimento di Scienze Farmaceutiche, Università degli Studi di Trieste, Piazzale Europa 1, 34127 Trieste, Italy, Departamento de Química Inorgánica, Orgánica y Bioquímica, Facultad de Químicas, Universidad de Castilla-La Mancha, Campus Universitario, 13071 Ciudad Real, Spain, Institut de Chimie, Université de Neuchâtel, Avenue de Bellevaux 51,CP 158, 2009 Neuchâtel, Switzerland, and Institute for Physical and Theoretical Chemistry, Friedrich-Alexander-Universität Erlangen-Nürnberg Universität Erlangen, Egerlandstrasse 3,91058 Erlangen, Germany

prato@units.it; robert.deschenaux@unine.ch; dirk.guldi@chemie.uni-erlangen.de

Received May 8, 2006

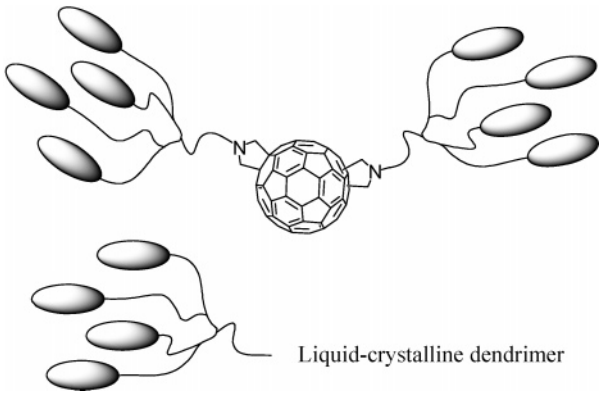

A second-generation cyanobiphenyl-based dendrimer was used as a liquid-crystalline promoter to synthesize mesomorphic bisadducts of [60]fullerene. Liquid-crystalline *trans*-2, *trans*-3, and equatorial bisadducts were obtained by condensation of the liquid-crystalline promoter, which carries a carboxylic acid function, with the corresponding bisaminofullerene derivatives. A monoadduct of fullerene was also prepared for comparative purposes. All the compounds gave rise to smectic A phases. An additional mesophase, which could not be identified, was observed for the *trans*-2 derivative. The supramolecular organization of the monoadduct derivative is governed by steric constraints. Indeed, for efficient space filling, adequacy between the cross-sectional areas of fullerene (∼100 Å^2) and of the mesogenic groups (∼22−25 Å^2 per mesogenic group) is required. As a consequence, the monoadduct forms a bilayered smectic A phase. The supramolecular organization of the bisadducts is essentially governed by the nature and structure of the mesogenic groups and dendritic core. Therefore, the bisadducts form monolayered smectic A phases. The title compounds are promising supramolecular materials as they combine the self-organizing behavior of liquid crystals with the properties of fullerene.

Introduction

Owing to its remarkable properties, [60]fullerene (C_{60}) is a valuable candidate for the preparation of functional dendrimers.[1−6] The functionalization of C_{60} with dendrimers increases its solubility in organic solvents and in water,[7] and the encapsula-

[†] Università degli Studi di Trieste.
[||] Universidad de Castilla-la Mancha.
[‡] Université de Neuchâtel.
[§] Friedrich-Alexander-Universität Erlangen-Nürnberg Universität Erlangen.

(1) Nierengarten, J.-F. *Chem.−Eur. J.* **2000**, *6*, 3667.
(2) Nierengarten, J.-F.; Armaroli, N.; Accorsi, G.; Rio, Y.; Eckert, J.-F. *Chem.−Eur. J.* **2003**, *9*, 36.
(3) Nierengarten, J.-F. *Top. Curr. Chem.* **2003**, *228*, 87.
(4) Hirsch, A.; Vostrowsky, O. *Top. Curr. Chem.* **2001**, *217*, 51.
(5) Chuard, T.; Deschenaux, R. *J. Mater. Chem.* **2002**, *12*, 1944.
(6) Jiang, D.-L.; Aida, T. *Prog. Polym. Sci.* **2005**, *30*, 403.
(7) Brettreich, M.; Hirsch, A. *Tetrahedron Lett.* **1998**, *39*, 2731.

10.1021/jo0609576 CCC: $33.50
Published on Web 09/06/2006

CHART 1

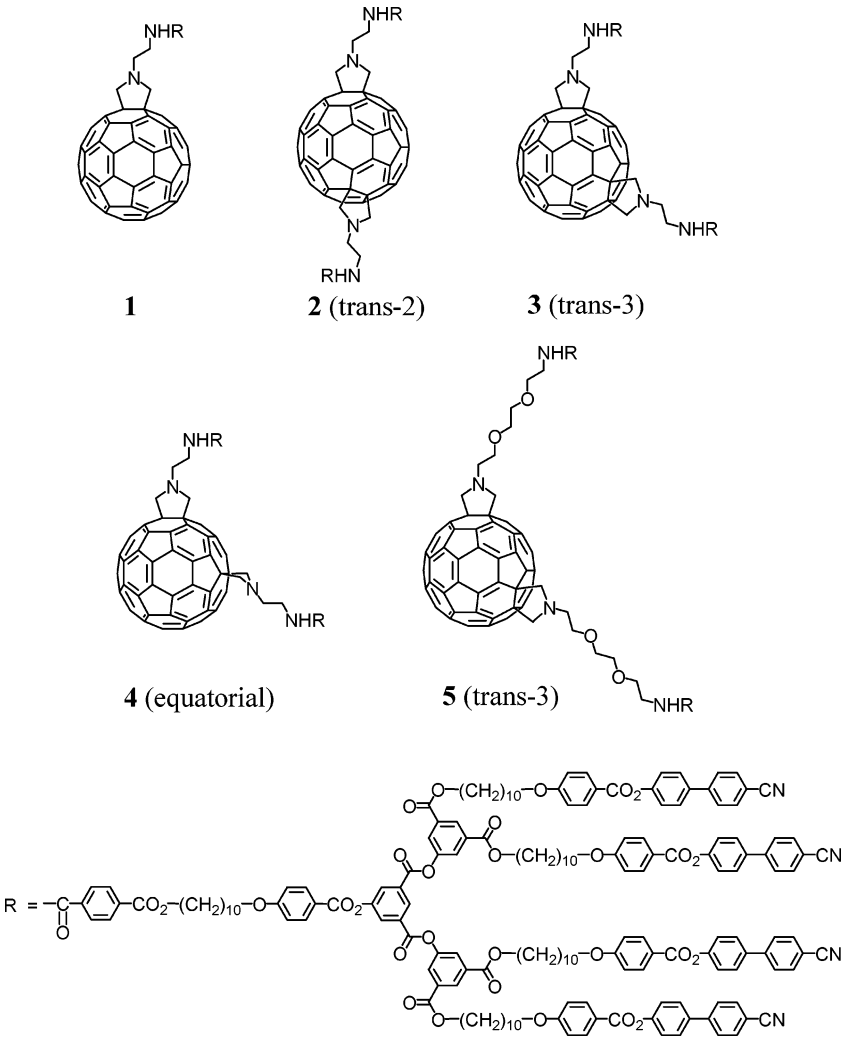

tion of C_{60} in dendritic matrices allows its protection from external chemicals, such as solvent molecules or molecular oxygen.[8−10] Dendrimers also prevent unfavorable interactions between the C_{60} units from taking place, which is of prime importance for the elaboration of supramolecular fullerene materials, such as Langmuir and Langmuir−Blodgett films[11−13] and liquid crystals.[5]

Addition of mesomorphic malonates to C_{60} via the Bingel reaction[14] led to liquid-crystalline methanofullerenes,[5,15,16] and 1,3-dipolar cycloaddition[17,18] of mesomorphic aldehydes and various *N*-substituted glycines to C_{60} yielded liquid-crystalline fulleropyrrolidines.[19−22] Contrary to the Bingel adducts, which undergo retro-addition upon chemical[23] and electrochemical reductions,[24−26] fulleropyrrolidines can accept up to five electrons without losing the organic addend. A retro-1,3-dipolar cycloaddition under chemical conditions was recently reported.[27]

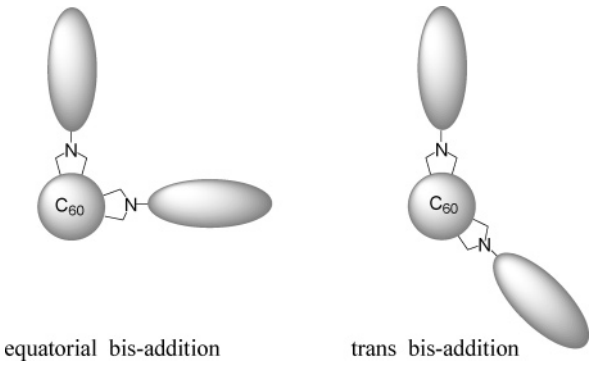

FIGURE 1. Pictorial structures of the positional isomers of C_{60}.

(8) Rio, Y.; Accorsi, G.; Nierengarten, H.; Rehspringer, J.-L.; Hönerlage, B.; Kopitkovas, G.; Chugreev, A.; Van Dorsselaer, A.; Armaroli, N.; Nierengarten, J.-F. *New J. Chem.* **2002**, *26*, 1146.

(9) Rio, Y.; Accorsi, G.; Nierengarten, H.; Bourgogne, C.; Strub, J.-M.; Van Dorsselaer, A.; Armaroli, N.; Nierengarten, J.-F. *Tetrahedron* **2003**, *59*, 3833.

(10) Kunieda, R.; Fujitsuka, M.; Ito, O.; Ito, M.; Murata, Y.; Komatsu, K. *J. Phys. Chem. B* **2002**, *106*, 7193.

(11) Cardullo, F.; Diederich, F.; Echegoyen, L.; Habicher, T.; Jayaraman, N.; Leblanc, R. M.; Stoddart, J. F.; Wang, S. *Langmuir* **1998**, *14*, 1955.

(12) Felder, D.; Gallani, J.-L.; Guillon, D.; Heinrich, B.; Nicoud, J.-F.; Nierengarten, J.-F. *Angew. Chem., Int. Ed.* **2000**, *39*, 201.

(13) Nierengarten, J.-F.; Eckert, J.-F.; Rio, Y.; del Pilar Carreon, M.; Gallani, J.-L.; Guillon, D. *J. Am. Chem. Soc.* **2001**, *123*, 9743.

(14) Bingel, C. *Chem. Ber.* **1993**, *126*, 1957.

(15) Campidelli, S.; Eng, C.; Saez, I. M.; Goodby, J. W.; Deschenaux, R. *Chem. Commun.* **2003**, 1520.

(16) (a) Even, M.; Heinrich, B.; Guillon, D.; Guldi, D. M.; Prato, M.; Deschenaux, R. *Chem. Eur. J.* **2001**, *7*, 2595. (b) Allard, E.; Oswald, F.; Donnio, B.; Guillon, D.; Delgado, J. L.; Langa, F.; Deschenaux, R. *Org. Lett.* **2005**, *7*, 383.

(17) Maggini, M.; Scorrano, G.; Prato, M. *J. Am. Chem. Soc.* **1993**, *115*, 9798.

SCHEME 1[a]

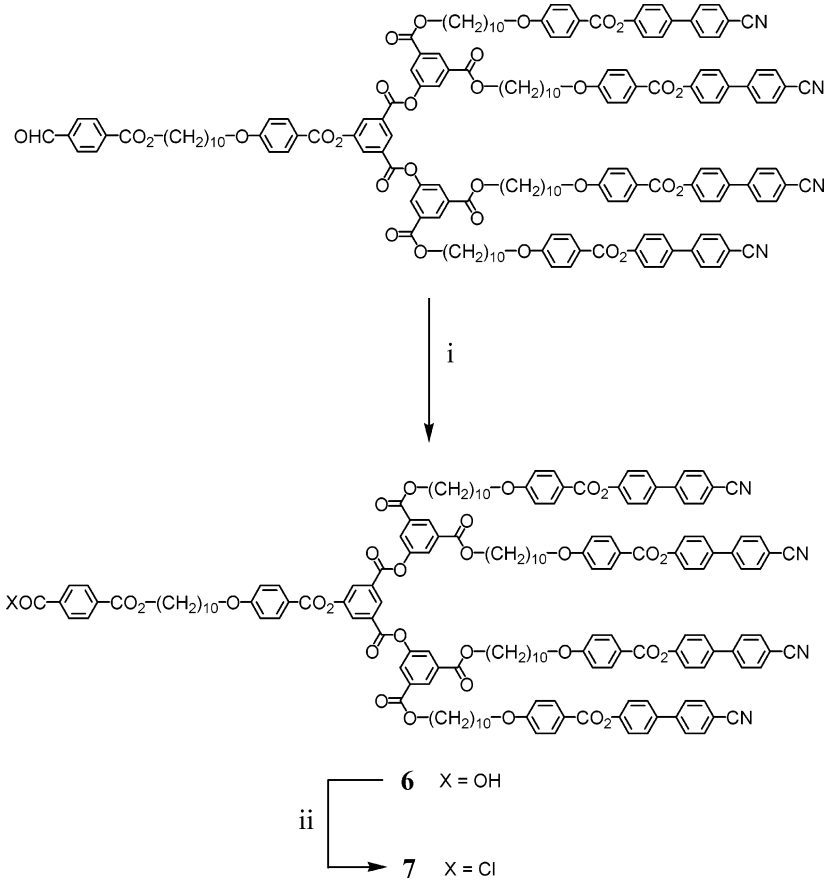

[a] Reagents and conditions: (i) sodium chlorite, sulfamic acid, THF/water, rt, quantitative yield; (ii) thionyl chloride, CH_2Cl_2, reflux, quantitative yield.

In most cases, the liquid-crystalline properties of the dendritic addends are transferred to C_{60} without drastic modifications of the mesomorphism. As an alternative approach to the monofunctionalization of C_{60}, the hexa-addition was also used to synthesize fullerene-containing liquid crystals.[28−30] This addition pattern can be used to obtain liquid-crystalline materials from nonmesomorphic addends. However, the major drawback of the hexa-addition pattern is that the properties of C_{60} are considerably altered. The design of liquid-crystalline multi-adducts of C_{60} functionalized with a reduced number of addends (compared with the hexa-adducts) represents a conceptual challenge. Indeed, such materials would display the self-organization behavior of liquid crystals and retain most of the properties of C_{60}. Mesomorphic bisadducts of C_{60} functionalized with dendritic addends as liquid-crystalline promoters are appealing compounds as they would meet these characteristics.

Most of the work on multiple additions is based on the cyclopropanation reaction. The same extensive amount of work has not been carried out for pyrrolidine adducts, even though the 1,3-dipolar cycloaddition of azomethine ylides to C_{60} is one of the most widely used functionalization of fullerenes. Recently, several papers reported the synthesis and characterization of bis- and trisadducts of fulleropyrrolidines.[31−35] Full separation and characterization of the eight bisadducts of fulleropyrrolidines allowed the assignment of each regioisomer based on symmetry considerations and on NMR spectroscopy using HMQC (Heteronuclear Multiple-Quantum Coherence) and HMBC (Heteronuclear Multiple Bond Correlation) techniques.[31] The bis-addition onto C_{60} may lead to a variety of interesting structures, including V-shaped structures with different angles (Figure 1).

(18) Prato, M.; Maggini, M. *Acc. Chem. Res.* **1998**, *31*, 519.
(19) Campidelli, S.; Deschenaux, R. *Helv. Chim. Acta* **2001**, *84*, 589.
(20) Campidelli, S.; Deschenaux, R.; Eckert, J.-F.; Guillon, D.; Nierengarten, J.-F. *Chem. Commun.* **2002**, 656.
(21) Campidelli, S.; Vázquez, E.; Milic, D.; Prato, M.; Barberá, J.; Guldi, D. M.; Marcaccio, M.; Paolucci, D.; Paolucci, F.; Deschenaux, R. *J. Mater. Chem.* **2004**, *14*, 1266.
(22) Campidelli, S.; Lenoble, J.; Barberá, J.; Paolucci, F.; Marcaccio, M.; Paolucci, D.; Deschenaux, R. *Macromolecules* **2005**, *38*, 7915.
(23) Moonen, N. N. P.; Thilgen, C.; Echegoyen, L.; Diederich, F. *Chem. Commun.* **2000**, 335.
(24) Kessinger, R.; Crassous, J.; Herrmann, A.; Rüttimann, M.; Echegoyen, L.; Diederich, F. *Angew. Chem., Int. Ed.* **1998**, *37*, 1919.
(25) Kessinger, R.; Fender, N. S.; Echegoyen, L. E.; Thilgen, C.; Echegoyen, L.; Diederich, F. *Chem.—Eur. J.* **2000**, *6*, 2184.
(26) Fender, N. S.; Nuber, B.; Schuster, D. I.; Wilson, S. R.; Echegoyen, L. *J. Chem. Soc., Perkin Trans. 2* **2000**, 1924.
(27) Martín, N.; Altable, M.; Filippone, S.; Martín-Domenech, A.; Echegoyen, L.; Cardona, C. M. *Angew. Chem., Int. Ed.* **2006**, *45*, 110.
(28) Chuard, T.; Deschenaux, R.; Hirsch, A.; Schönberger, H. *Chem. Commun.* **1999**, 2103.
(29) Tirelli, N.; Cardullo, F.; Habicher, T.; Suter, U. W.; Diederich, F. *J. Chem. Soc., Perkin Trans. 2* **2000**, 193.
(30) Felder-Flesch, D.; Rupnicki, L.; Bourgogne, C.; Donnio, B.; Guillon, D. *J. Mater. Chem.* **2006**, *16*, 304.
(31) Kordatos, K.; Bosi, S.; Da Ros, T.; Zambon, A.; Lucchini, V.; Prato, M. *J. Org. Chem.* **2001**, *66*, 2802.
(32) Nakamura, Y.; O-kawa, K.; Nishimura, T.; Yashima, E.; Nishimura, J. *J. Org. Chem.* **2003**, *68*, 3251.
(33) Nishimura, T.; Tsuchiya, K.; Ohsawa, S.; Maeda, K.; Yashima, E.; Nakamura, Y.; Nishimura, J. *J. Am. Chem. Soc.* **2004**, *126*, 11711.
(34) Marchesan, S.; Da Ros, T.; Prato, M. *J. Org. Chem.* **2005**, *70*, 4706.
(35) Zhou, Z.; Schuster, D. I.; Wilson, S. R. *J. Org. Chem.* **2006**, *71*, 1545.

SCHEME 2 [a]

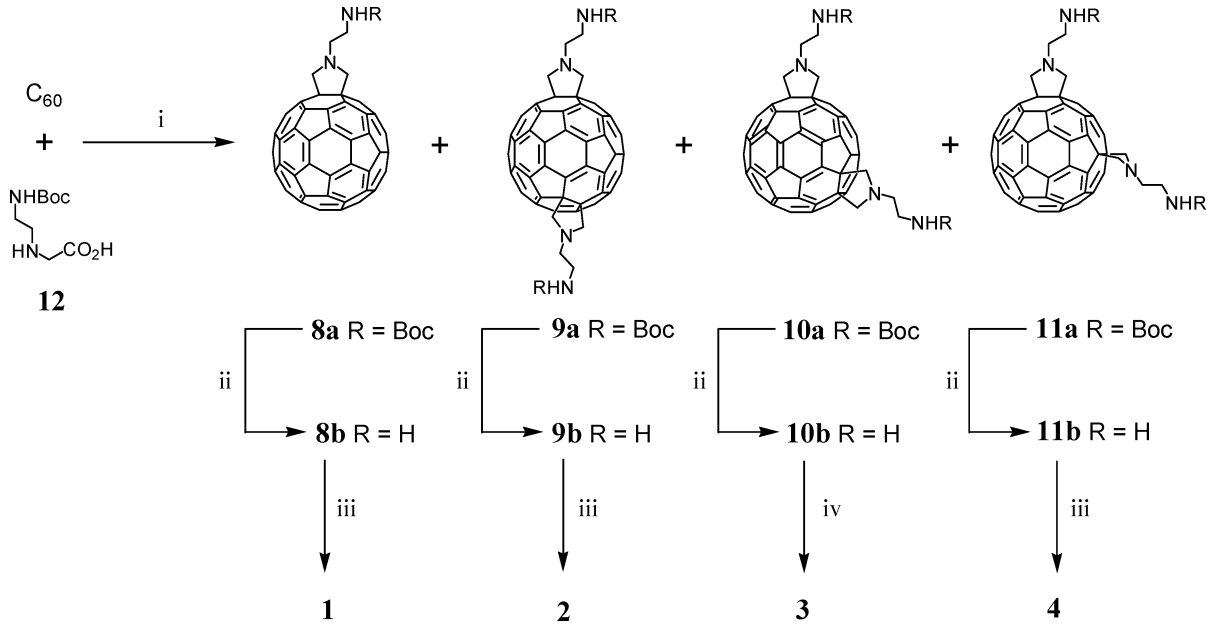

[a] Reagents and conditions: (i) paraformaldehyde, toluene, reflux, yield: **8a** (29%), **9a** (3.6%), **10a** (5.8%), and **11a** (3.1%); (ii) trifluoroacetic acid, CH_2Cl_2, rt, quantitative yield; (iii) acid chloride **7**, Et_3N, CH_2Cl_2, rt, yield: **1** (19%), **2** (13%), and **4** (17%); (iv) acid **6**, EDC, HOBt, Et_3N, CH_2Cl_2, rt, 9%.

SCHEME 3 [a]

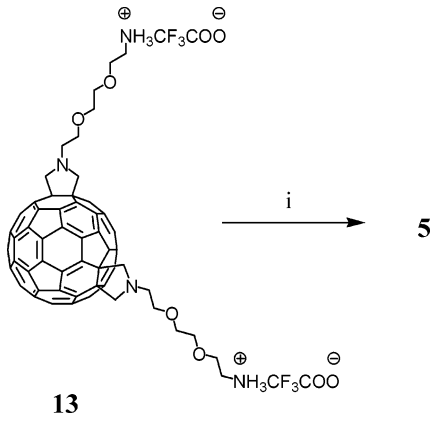

[a] Reagents and conditions: (i) **6**, EDC, HOBt, Et_3N, CH_2Cl_2, rt, 15%.

With the view to exploit C_{60} as a synthetic platform for the design of liquid-crystalline materials and explore the behavior of liquid crystals with uncoventional shapes, we decided to investigate the mesomorphic properties of fullerodendrimers based on the bis-addition pattern. We describe, herein, the synthesis, characterization, liquid-crystalline behavior, supramolecular organization, and photophysical properties of monoadduct **1**, which is used for comparative purposes, and bisadducts **2**−**5**. A second-generation cyanobiphenyl-based dendrimer was selected as the liquid-crystalline promoter. Compounds **2**, **3**, and **4** were designed to study the influence of the position of the addends on the mesomorphism, and **5** was synthesized to examine if the length of the spacer influences the mesomorphic behavior and/or the supramolecular organization of the resulting material.

Results and Discussion

The structures of the compounds investigated in this paper (a monoadduct **1** and four bisadducts **2**−**5**) are shown in Chart 1.

Synthetic Concept. The synthetic strategy applied is based on the preparation and isolation of mono- and bisamine intermediates, followed by grafting of the liquid-crystalline promoter onto the amine functions.

Synthesis. The synthesis of the liquid-crystalline dendrimers **6** and **7** is described in Scheme 1. Dendrimer **6** was prepared by oxidation of the corresponding aldehyde derivative[22] in the presence of sodium chlorite and sulfamic acid in a mixture of THF and water. Reaction of **6** with thionyl chloride in dry CH_2Cl_2 yielded **7**.

The preparation of **1**−**4** is presented in Scheme 2. Fullerene derivatives **8a**−**11a** were prepared by 1,3-dipolar cycloaddition from **12**[36] (2 equiv), paraformaldehyde (5 equiv), and C_{60} (1 equiv) in toluene (under reflux). Monoadduct **8a** was easily separated by column chromatography from unreacted C_{60} and the bisadducts. Isolation of regioisomers **9a**−**11a** required a second separation by column chromatography. The order of elution was *trans*-2 **9a**, *trans*-3 **10a**, and, finally, equatorial **11a**. The amine groups of **8a**−**11a** were deprotected by trifluoroacetic acid in CH_2Cl_2 to give the protonated amines **8b**−**11b**. Reaction of **8b**, **9b**, and **11b** with acid chloride **7** in the presence of Et_3N led to **1**, **2**, and **4**, respectively. Under similar reaction conditions, bisadduct **3** (from **10b**) could not be isolated since the reaction did not proceed to a sufficient extent; it was obtained by condensation of carboxylic acid **6** with **10b** in the presence of *N*-(3-dimethylaminopropyl)-*N*′-ethylcarbodiimide (EDC), 1-hydroxybenzotriazole (HOBt), and Et_3N.

The synthesis of **5** was achieved by reaction of **13**[37] with **6** in the presence of EDC, HOBt, and Et_3N (Scheme 3).

All compounds, except **8b**−**11b**, which are insoluble in organic solvents, were characterized by NMR spectroscopy and mass spectrometry (see Experimental Section and Supporting

(36) Kordatos, K.; Da Ros, T.; Bosi, S.; Vázquez, E.; Bergamin, M.; Cusan, C.; Pellarini, F.; Tomberli, V.; Baiti, B.; Pantarotto, D.; Georgakilas, V.; Spalluto, G.; Prato, M. *J. Org. Chem.* **2001**, *66*, 4915.

(37) Bosi, S.; Feruglio, L.; Milic, D.; Prato, M. *Eur. J. Org. Chem.* **2003**, 4741.

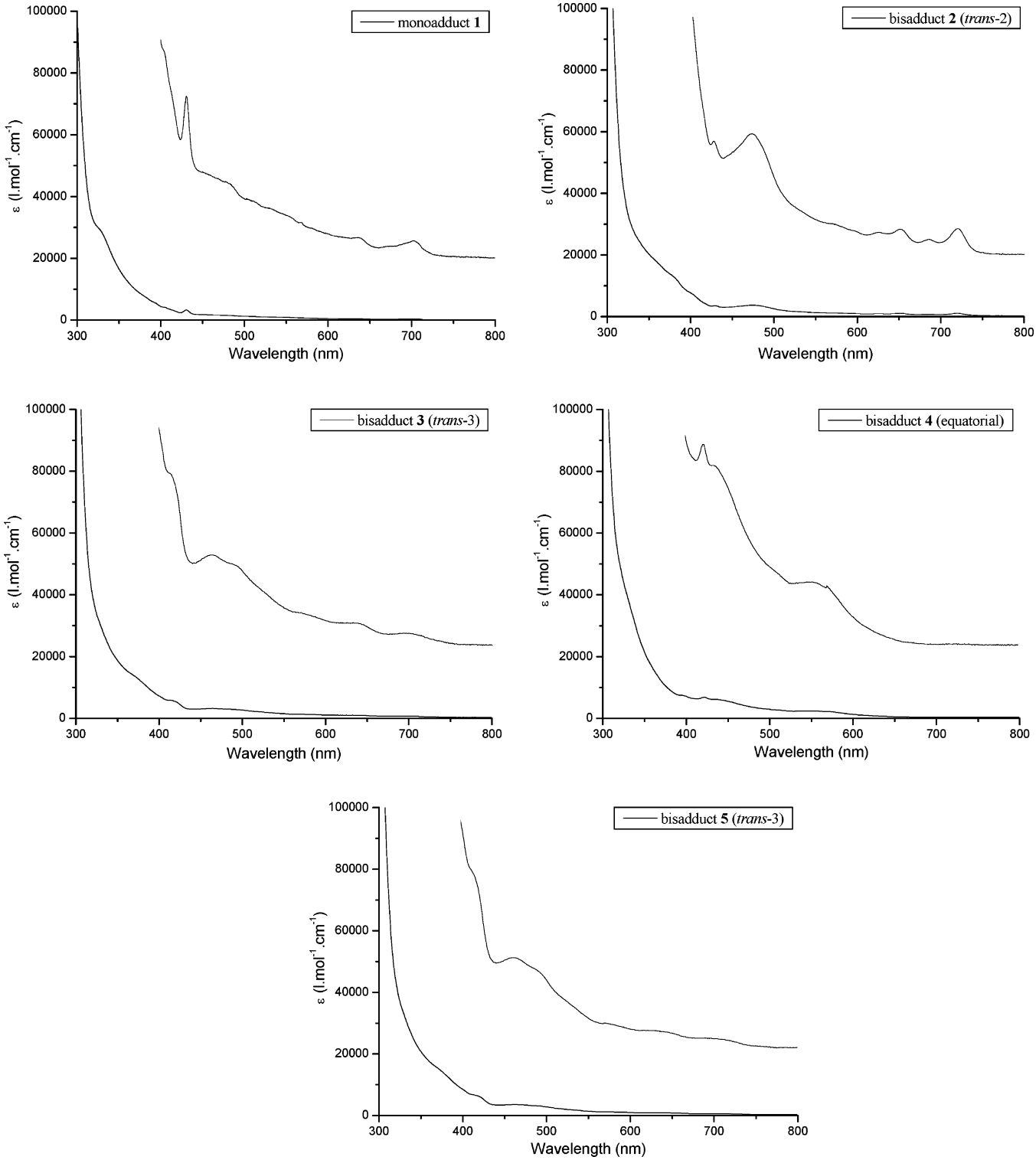

FIGURE 2. UV−vis spectra of **1**−**5**.

Information). The structures of mono- and bisadducts of C_{60} were confirmed by UV−vis spectroscopy (Figure 2) from the observation of characteristic absorption peaks: monoadduct **1** shows two maxima at 431 and 703 nm, bisadduct *trans*-2 **2** presents six maxima at 429, 475, 626, 651, 686, and 720 nm, bisadducts *trans*-3 **3** and equatorial **4** show only two maxima at 464 and 695, and at 421 and 552 nm, respectively. Finally, bisadduct *trans*-3 **5** exhibits only one maximum at 462 nm. The UV−vis spectra are in agreement with previous studies.[31,38]

Liquid-Crystalline Properties. The mesomorphic and thermal properties of **1**−**6** were investigated by polarized optical microscopy (POM) and differential scanning calorimetry (DSC). The phase transition temperatures and enthalpies are reported in Table 1.

(38) Kordatos, K.; Da Ros, T.; Prato, M.; Bensasson, R. V.; Leach, S. *Chem. Phys.* **2003**, *293*, 263.

TABLE 1. Phase Transition Temperatures[a] and Enthalpy Changes of Compounds 1−6

compound	T_g (°C)	transition	T (°C)	ΔH (kJ/mol)
1		Cr → S_A	44	3.2
		S_A → I	153	7.6
2	60	S_A → M	167	
		M → I	170	13.1[b]
3	61	S_A → I	169	13.4
4		Cr → S_A	42	8.0
		S_A → I	166	16.0
5	52	S_A → I	161	15.8
6	45	S_A → I	203	18.6

[a] T_g = glass transition temperature, Cr = semicrystalline solid, S_A = smectic A phase, I = isotropic liquid, M = unidentified mesophase. Temperatures are given as the onset of the peak obtained during the second heating run. T_g values are determined during the first cooling run. [b] Overall enthalpy.

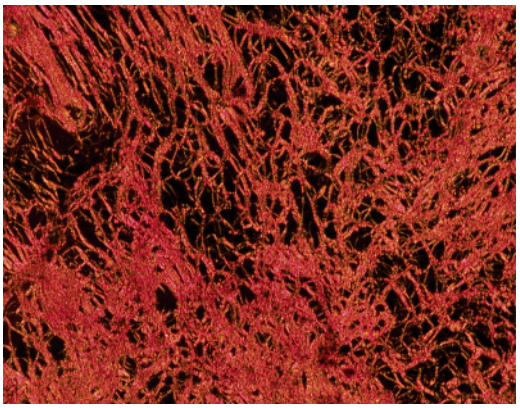

FIGURE 3. Thermal polarized optical micrograph of the focal-conic and homeotropic textures displayed by **2** at 151 °C.

All compounds displayed smectic A (S_A) phases, which were identified by POM from the observation of typical focal-conic and homeotropic textures. Bisadduct *trans*-2 **2** gave an additional short-range mesophase between the smectic A phase and the isotropic liquid. This mesophase formed on heating and cooling the sample but could not be identified by POM as a typical texture could not be obtained under the various experimental conditions applied. Only an optically isotropic or homeotropic texture was observed, which was indicative of the formation of a nematic phase or more sophisticated mesophases, such as cubic phases. Unambiguous characterization of this mesophase requires investigations by X-ray diffraction techniques. However, the small amount of compound synthesized did not allow us to carry out such experiments. The textures of the smectic A phase developed by **2** are shown in Figure 3 as an illustrative example.

The clearing points of the fullerenes were found to be about 30−50 °C lower than the one of the acid precursor. This result can be explained from structural considerations: for the monoadduct, the second-generation dendrimer is not large enough to compensate the bulkiness of C_{60}, which acts as a spacer, and so it decreases the intermolecular attractions. For the bisadducts, the influence of C_{60} is reduced but still present.[5,22] Comparison of the clearing points between the monoadduct **1** and the bisadducts **2**−**4** shows that the stability of the mesophases increases with the number of mesogenic groups as a consequence of stronger intermolecular interactions. Comparison of the clearing points between bisadducts *trans*-3 **3** and *trans*-3 **5** shows that the stability of the mesophase increases when the length of the spacer decreases. This result should be the consequence of reduced molecular motion when the spacer is shorter. Finally, the formation of the smectic A phases observed for **1**−**6** is in agreement with the nature of the

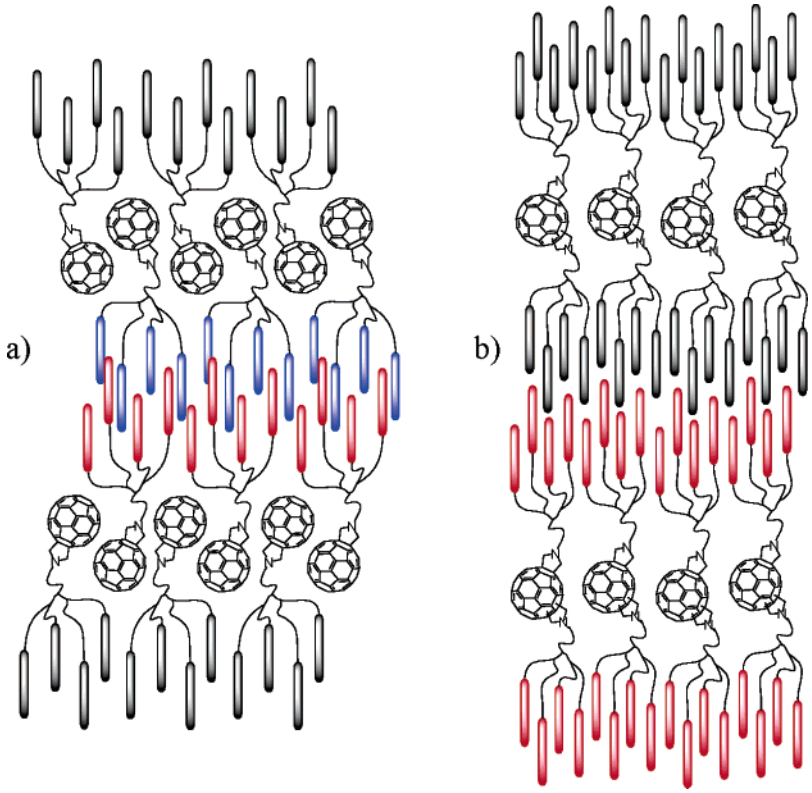

FIGURE 4. Postulated supramolecular organization of (a) monoadduct **1** and (b) bisadducts **2**−**5** within the smectic A phase.

TABLE 2. Summary of the Spectroscopic Data for 1−4

	1 mono	**2** *trans*-2	**3** *trans*-3	**4** equatorial
fluorescence maximum	710 nm	690 nm	720 nm	690 nm
fluorescence quantum yield	6.0×10^{-4}	10.5×10^{-4}	4.5×10^{-4}	1.6×10^{-4}
fluorescence lifetime	0.72 ns	0.76 ns	0.90 ns	0.98 ns
singlet−singlet maximum	890 nm	900 nm	900 nm	940 nm
singlet excited state lifetime	0.98 ns	0.76 ns	1.02 ns	1.01 ns
triplet−triplet maximum	700 nm	670 nm	650 nm	680 nm
triplet excited state lifetime	11.0 μs	16.0 μs	7.2 μs	3.5 μs

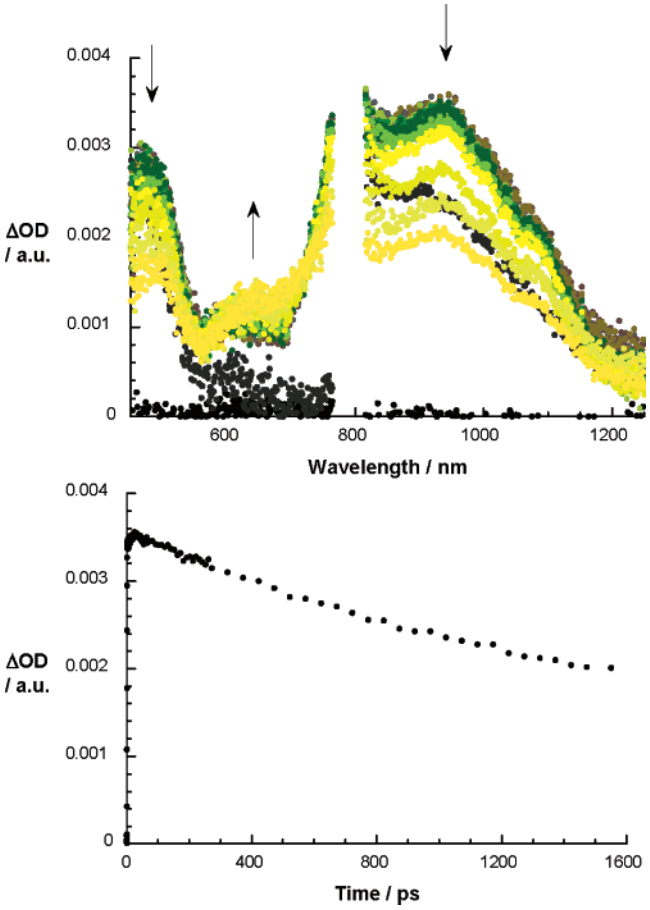

FIGURE 5. Top: differential absorption spectra (visible and near-infrared) obtained upon femtosecond flash photolysis (387 nm) of the equatorial bisadduct **4** in deoxygenated dichloromethane with several time delays between 0 and 1500 ps at room temperature. Bottom: time absorption profiles of the spectra shown above at 950 nm.

dendromesogens, which have a strong tendency to align parallel one to each other and so give rise to the formation of layers.[22,39]

Supramolecular Organization. For monoadduct **1**, the molecular organization within the smectic layers is essentially governed by steric factors, that is, the required adequacy between the cross-sectional areas of C_{60} (90−100 Å^2) and that of the mesogenic units (22−25 Å^2 per mesogenic unit). Thus, the cyanobiphenyl units of one molecule point in the same direction, and the molecules are organized in a head-to-tail fashion, forming a bilayered smectic A phase (Figure 4a).

For bisadducts **2**−**5**, two dendrons are located on the C_{60} sphere. The dendrimers expand laterally with respect to C_{60}. Therefore, C_{60} is embedded in the middle of the layers formed by the cyanobiphenyl-based dendrimers and has no influence

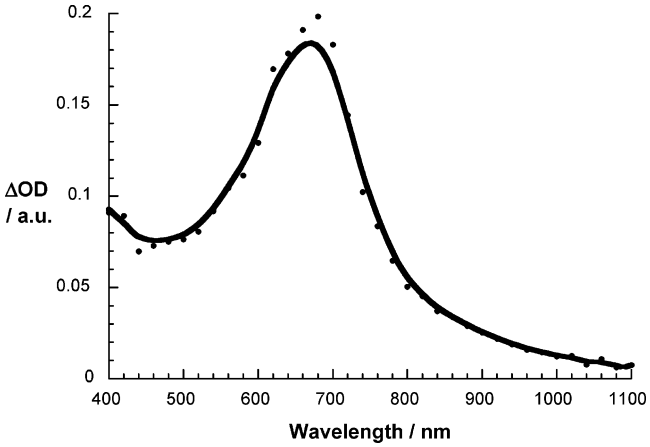

FIGURE 6. Transient triplet excited state spectrum (obtained upon nanosecond flash photolysis at 355 nm) of the equatorial bisadduct **4** in deoxygenated dichloromethane with a time delay of 50 ns.

on the supramolecular organization. The bisadduct derivatives are organized into a monolayered smectic A phase, similar to that obtained for fulleropyrrolidines and methanofullerenes functionalized by analogous liquid-crystalline dendrimers.[22,39] For **2**−**5**, the supramolecular organization is essentially governed by the nature and structure of the mesogenic units and of the dendritic core. The postulated organization of the bisadducts within the smectic A phase is shown in Figure 4b.

Photophysical Properties. The mono- and bisadduct derivatives **1**−**4** were probed—as deoxygenated dichloromethane solutions—in a series of photophysical experiments. In particular, we tested them by steady-state/time-resolved fluorescence spectroscopy and time-resolved transient absorption spectroscopy. A summary of all spectroscopic data is given in Table 2.

First, let us examine the steady-state fluorescence spectra. Excitation in the visible region (i.e., 380 nm) leads, for **1**−**3**, to the typical fullerene fluorescence spectrum with maxima in the 650−690 nm range. Only the equatorial bisadduct **4** deviates from that. This is, however, in line with previous observations that were made with several equatorial bisadducts (i.e., fulleropyrrolidines and methanofullerenes).[40] Complementary to these steady-state investigations, we followed the fluorescence decays of the singlet excited states (**1**−**4**) and their corresponding fluorescence maxima. Hereby, a short (800 ps) laser excitation at 337 nm was utilized. The lifetimes were around 1 ns, which is somewhat shorter than what is typically found in mono- and bisadduct derivatives of C_{60}.

The weak fluorescence of **1**−**4** is overshadowed by an effective intersystem crossing between the singlet excited states and the corresponding triplet manifolds. Such information is derived from transient absorption spectroscopy utilizing femtosecond (i.e., 150 fs) excitation at 387 nm. Common to all derivatives are singlet−singlet features in the near-infrared region, that is, around 900 nm. The singlet excited state transients decay on the time scale of our femtosecond experiments (i.e., 1.5 ns). Parallel to this decay, we see the growth of the triplet−triplet characteristics (vide infra). The latter are blue-shifted relative to the singlet−singlet absorptions (Figure 5).

(39) Dardel, B.; Guillon, D.; Heinrich, B.; Deschenaux, R. *J. Mater. Chem.* **2001**, *11*, 2814.

(40) (a) Guldi, D. M.; Prato, M. *Acc. Chem. Res.* **2000**, *33*, 695. (b) Guldi, D. M.; Hungerbühler, H.; Asmus, K.-D. *J. Phys. Chem.* **1995**, *99*, 9380.

The final set of experiments dealt with the same triplet excited state features, which were generated with nanosecond (i.e., 6 ns) excitation at 355 nm. These experiments shed light into the dynamics that might evolve from a feasible aggregation in solution. For instance, clustering of fullerenes is known to lead to instantaneous triplet−triplet annihilation, while in monomeric fullerenes, the lifetime extends well into the tenth of microseconds. Compounds **1**−**4** exhibit triplet−triplet absorptions that agree well with previously reported features, namely, maxima in the 690−710 nm range (Figure 6). Moreover, decay rates of around 10^5 s^{-1} support the notion that **1**−**4** exist in their monomeric configuration without significant C_{60}−C_{60} interactions.

Conclusion

We have described the synthesis, characterization, properties, and supramolecular organization of liquid-crystalline fullerene bisadducts **2**−**5** and monoadduct **1** used as reference compound. All compounds displayed smectic A phases. The *trans*-2 bisadduct **2** showed an additional short-range mesophase which could not be identified. On the basis of structural considerations, we postulated that the mono- and bisadducts formed bilayered and monolayered smectic A phases, respectively. The title compounds are interesting materials as they combine the self-organizing behavior of liquid crystals and retain most of the properties of [60]fullerene. A comprehensive investigation of the physicochemical properties of **1**−**4** confirms that in these novel fullerene derivatives the basic fullerene features are largely preserved. Importantly, no spectroscopic evidence for strong $\pi-\pi$ interactions between individual fullerenes was found.

Experimental Section

Compounds **12**[36] and **13**[37] were prepared according to literature procedures.

General Procedure for the Synthesis of 8a−11a. A solution of C_{60} (909 mg, 1.261 mmol), paraformaldehyde (189 mg, 6.307 mmol), and **12**[36] (551 mg, 2.523 mmol) in toluene (650 mL) was heated under reflux for 2.5 h. The solution was concentrated under reduced pressure, and the monoadduct **8a** was purified from unreacted C_{60}, bis-, and higher adducts by column chromatography (silica gel, 63−200 μm), eluting first with toluene (to recover C_{60}) and then with a mixture of toluene/ethyl acetate 97:3. Precipitation of **8a** from a CS_2 solution with Et_2O and subsequent washing with Et_2O gave pure **8a**. The bisadducts were eluted with a mixture of toluene/ethyl acetate 50:50 and purified by a second column chromatography (silica gel, 15−40 μm) with toluene/ethyl acetate first 97:3 and then by a slow increase of polarity up to 80:20. The order of elution is *trans*-2, *trans*-3, and equatorial. Precipitation of the bisadducts from a CH_2Cl_2 solution with hexane gave pure compounds.

8a (mono): (334 mg, 29%). ^{1}H NMR (200 MHz, $CDCl_3 + CS_2$) δ (ppm) 5.37−5.16 (br s, 1H, NH), 4.46 (s, 4H, pyrrolidine), 3.72−3.63 (m, 2H, C*H*$_2$NHBoc), 3.24 (t, 2H, NCH_2), 1.50 (s, 9H, Boc). ^{13}C NMR (50 MHz, $CDCl_3 + CS_2$): δ (ppm) 156.0, 154.8, 147.3, 146.3, 146.1, 146.0, 145.7, 145.5, 145.3, 144.6, 143.2, 142.7, 142.2, 142.1, 142.0, 140.2, 136.3, 78.8, 70.7, 67.9, 54.4, 28.6. IR-DRIFT (KBr): ν (cm^{-1}) 3333, 2967, 1704, 1520, 1255, 1172, 770, 523. UV−vis (CH_2Cl_2): λ_{max} (nm) 256, 329, 430, 703. ES-MS: *m*/*z* 907 (MH^+).

General Procedure for the Synthesis of 8b−11b. Trifluoroacetic acid (TFA) was added to a solution of the Boc derivative in CH_2Cl_2. The solution was stirred at room temperature and under N_2 for 1 h. The reaction mixture was evaporated, and traces of TFA were removed by adding toluene and evaporating the solution to dryness (several times). Compounds **8b**−**11b** were purified by precipitation from a MeOH solution with Et_2O.

8b: from **8a** (153 mg, 0.168 mmol), TFA (3 mL), CH_2Cl_2 (3 mL); **8b** (155 mg, quantitative yield). IR-DRIFT (KBr): ν (cm^{-1}) 3108−2787, 1678, 1202, 1133, 721, 526. UV−vis (THF): λ_{max} (nm) 255, 326, 431, 704. ES-MS: *m*/*z* 806 (M^+).

Compound 2. To a solution of **9b** (20 mg, 0.018 mmol) and Et_3N (300 μL) in dry CH_2Cl_2 (3 mL) at 0 °C was added a solution of freshly prepared **7** (100 mg, 0.036 mmol) in dry CH_2Cl_2 (4 mL). The reaction was stirred for 2 h at room temperature, and the solvent was removed. Purification of the crude material by column chromatography (silica gel 63−200 μm, toluene/ethyl acetate 8:2) and precipitation from CH_2Cl_2 with MeOH gave pure **2** (15 mg, 13%). ^{1}H NMR (200 MHz, $CDCl_3$): δ (ppm) 8.95 (t, 2H, arom. H), 8.65 (t, 4H, arom. H), 8.37 (d, 4H, arom. H), 8.24−8.02 (m, 36H, arom. H), 7.81−7.50 (m, 50H, arom. H and NH), 7.39−7.27 (m, 16H, arom. H), 6.99 (d, 20H, arom. H), 4.78 (d, 2H, pyrrolidine), 4.60 (d, 2H, pyrrolidine), 4.50−4.24 (m, 24H, CO_2-CH_2 and pyrrolidine), 4.12−3.95 (m, 24H, CH_2O and C*H*$_2$NH), 3.58−3.40 (m, 4H, NCH_2), 1.92−1.69 (m, 40H, $CO_2CH_2CH_2$ and C*H*$_2$$CH_2O$), 1.58−1.28 (m, 120H, aliph. H). ^{13}C NMR (50 MHz, $CDCl_3$): δ 166.4, 165.7, 164.7, 164.7, 163.6, 162.9, 152.9, 152.7, 151.5, 151.5, 150.4, 147.0, 145.6, 144.7, 143.6, 142.5, 141.3, 138.2, 137.0, 136.6, 133.7, 132.5, 132.2, 131.0, 129.8, 128.2, 127.6, 127.1, 126.9, 125.1, 123.6, 122.5, 121.1, 120.2, 118.8, 114.5, 114.3, 110.9, 69.2, 69.1, 68.3, 65.8, 50.9, 40.4, 29.5, 29.3, 29.2, 29.1, 28.6, 26.0. IR-DRIFT (KBr): ν (cm^{-1}) 3071, 2933, 2854, 2224, 1731, 1604, 1509, 1252, 1065, 1006, 844, 762, 533, 425. UV−vis (CH_2Cl_2): λ_{max} (nm) 277, 429, 475, 626, 651, 686, 720.

Compound 3. To a solution of **6** (147 mg, 0.053 mmol), HOBt (14 mg, 0.107 mmol), and EDC (20 mg, 0.107 mmol) in CH_2Cl_2 (6 mL) was added after 15 min a solution of **10b** (20 mg, 0.018 mmol) and Et_3N (300 μL) in CH_2Cl_2 (2 mL). The reaction was stirred overnight at room temperature, and then the solvent was removed. Purification of the crude material by column chromatography (silica gel 63−200 μm, toluene/ethyl acetate 10:0.5 to 10:1) and precipitation from CH_2Cl_2 with MeOH gave pure **3** (10 mg, 9%). ^{1}H NMR (200 MHz, $CDCl_3$): δ (ppm) 8.91 (t, 2H, arom. H), 8.61 (t, 4H, arom. H), 8.33 (d, 4H, arom. H), 8.21−8.06 (m, 28H, arom. H), 8.04 (d, 4H, arom. H), 7.91 (d, 4H, arom. H), 7.77−7.54 (m, 48H, arom. H), 7.40−7.20 (m, 18H, arom. H and NH), 6.95 (d, 20H, arom. H), 4.53−4.08 (series of m, 28H, CO_2CH_2 and pyrrolidine), 4.01 (t, 20H, CH_2O), 4.00−3.90 (m, 4H, C*H*$_2$-NH), 3.38−3.25 (m, 4H, NCH_2), 1.88−1.64 (m, 40H, $CO_2CH_2CH_2$ and C*H*$_2$$CH_2O$), 1.53−1.19 (m, 120H, aliph. H). ^{13}C NMR (50 MHz, $CDCl_3$): δ 165.7, 164.8, 163.6, 151.5, 150.4, 148.9, 147.4, 144.8, 136.6, 136.1, 132.6, 132.3, 129.7, 129.0, 128.2, 127.6, 126.9, 122.5, 121.1, 118.8, 114.3, 110.9, 68.3, 65.8, 29.5, 29.0, 28.7, 26.0. IR-DRIFT (KBr): ν (cm^{-1}) 3063, 2927, 2859, 2225, 1727, 1602, 1501, 1252, 1064, 998, 843, 756, 533, 434. UV−vis (CH_2Cl_2): λ_{max} (nm) 277, 464, 695.

Acknowledgment. This work was carried out with partial support from the University of Trieste, MIUR (PRIN 2004, prot. 2004035502), EU (RTN networks "WONDERFULL" and "FAMOUS"), SFB 583, DFG (GU 517/4-1), FCI, the Office of Basic Energy Sciences of the U.S. Department of Energy (NDRL 4683), and the Swiss National Science Foundation (Grant Nos. PBNE2-106767 and 200020-103424).

Supporting Information Available: ^{1}H and ^{13}C NMR spectra of **1**−**6**, **8a**, **9a**, **10a**, and **11a**, mass spectra of **8a**, **8b**, **9a**, **9b**, **10a**, **10b**, **11a**, and **11b**, and fluorescence and transient absorption spectra of **1**−**4**; experimental details for the preparation of **1**, **4**, **5**, **6**, and **7**; spectroscopic data of **9a**−**11a** and **9b**−**11b**. This material is available free of charge via the Internet at http://pubs.acs.org.

JO0609576